DOI: 10.1002/ejic.200800486

Cu^{2+}-Mediated Nucleophilic Addition of Different Nucleophiles to Dicyanamide – Synthesis, Structures, and Magnetic Properties of a Family of Mononuclear, Trinuclear, Hexanuclear, and Polymeric Copper(II) Complexes

Ling-Ling Zheng,[a] Ji-Dong Leng,[a] Wen-Ting Liu,[a] Wei-Xiong Zhang,[a] Jun-Xian Lu,[a] and Ming-Liang Tong*[a]

Keywords: Copper(II) / Polydentate ligands / Nucleophilic addition / Magnetic properties

Five new copper(II) complexes have been isolated from the reaction system of $Cu^{II}/N(CN)_2^-/HNu$ (HNu = pyrazole or MeOH) by Cu^{2+}-mediated in situ nucleophilic additions of methanol or pyrazole to dicyanamide; they are $[Cu(HdcadMeOH)_2](ClO_4)_2{\cdot}2H_2O$ (**3**), $[Cu(dca)_2(3\text{-nic})_2]_n{\cdot}(HdcaMeOH)_{2n}$ (**4**), [Cu(dcapz)(dcadMeOH)] (**5**), $[Cu_3(dcadpz)_2(Hpz)_2(MeCN)_2](ClO_4)_2(NO_3)_2$ (**6**), and $[Cu_6(dcadpz\text{-}2H)_2(\mu\text{-}pz)_6]$ (**7**) [HdcadMeOH = bis(methoxycarbimido)amine, HdcaMeOH = (methoxycarbimido)cyanoamine, $dcadMeOH^-$ = bis(methoxycarbimido)aminato, $dcapz^-$ = (pyrazolecarbimido)cyanoaminato, $dcadpz^-$ = bis(pyrazolecarbimido)aminato, Hpz = pyrazole, 3-nic = nicotinamide]. X-ray crystallography revealed that **3** and **5** are mononuclear complexes, **6** is a trinuclear complex, **7** is a cyclic hexanuclear cluster, whereas **4** is composed of neutral one-dimensional $[Cu(\mu_{1,5}\text{-}dca)_2(3\text{-nic})_2]_n$ coordination chains with HdcaMeOH guest molecules located between these chains. In the five complexes, the 1:1 and 1:2 nucleophilic addition reactions occurred between dca^- and methanol or pyrazole molecules under controlled conditions. In complexes **3**, **5**, **6**, and **7**, the addition products generated in situ act as bridging or chelating ligands, whereas in compound **4** the addition product acts as the guest molecule. The magnetic properties of complexes **6** and **7** were studied by variable-temperature magnetic susceptibility and magnetization measurements. In **6**, significant ferromagnetic coupling exists between the three $S = 1/2$ spins within the Cu_3 unit through the $dcadpz^-$ bridges, whereas in **7**, strong antiferromagnetic couplings exist between the neighboring copper ions through the $[dcadpz\text{-}2H]^{3-}$ and pz^- bridges with an intratrimer exchange interaction of –250.6 K and an intertrimer coupling interaction of –69.1 K.

(© Wiley-VCH Verlag GmbH & Co. KGaA, 69451 Weinheim, Germany, 2008)

Introduction

The metal-mediated and/or metal-catalyzed reactions of RCN species have been surveyed in a number of articles including previous reviews[1] and text-book considerations[2] on nitrile reactivity and also certain sections in recent general reviews on the reactivity of RCN ligands.[3] In the past decade, some reviews devoted exclusively to hydrolysis involving metal centers have been published, and they covered hydrolytic conversion occurring mainly at Ru, Re, and Pt centers.[4] Some recent reviews concern nitrile hydratases or mimetics of these enzymes.[5] In view of the increasing importance of metal-mediated hydrolysis to organonitriles for both coordination and organic chemistry, a critical investigation that covers hydrolytic conversions at various metal centers was thought to be timely.

Sodium dicyanamide [dca, $N(CN)_2^-$] has been extensively used in recent years to generate a wide variety of polymers of different topologies and magnetic properties.[6] However, what interests us is the nucleophilic addition of some nucleophiles to dicyanamide.[7–12] In our previous attempts to synthesize coordination polymers[13] with transition-metal(II) ions, Na(dca) and pyrazole (Hpz), a functional pentadentate ligand, bis(pyrazolecarbimido)aminate ($dcadpz^-$), was generated by a 2:1 nucleophilic addition of pyrazole to dicyanamide, which led to in-situ synthesis of a ferromagnetic homotrinuclear copper(II) cluster of $[Cu_3(dcadpz)_2(Hpz)_2(ClO_4)_2](ClO_4)_2{\cdot}H_2O$ (**1**), from which the interesting metalloligand $[Cu(dcadpz)_2]$ (**2α**) was isolated.[14] Subsequently, we isolated and characterized the free pentadentate ligand and two mononuclear precursors, $[Cu(dcadpz)_2]$ and $[Ni(dcadpz)_2]{\cdot}2/3dmf$, which were successfully used to rationally assemble a series of linear homo- and heterotrinuclear metal complexes, $[\{M(pdm)\}_2\{Cu(dcadpz)_2\}](NO_3)_4$ (M = Co and Ni; pdm = 2,6-pyridinedimethanol) and $[\{Ni(MeOH)(H_2O)_2\}_2\{Ni(dcadpz)_2\}](NO_3)_4$.[15a] Igashira-Kamiyama and co-workers applied the polymorphous mononuclear $[Cu(dcadpz)_2]$ (**2β**) precursor obtained in a mixed $EtOH/CHCl_3$ solution, to synthesize four linear tri-

---

[a] MOE Key Laboratory of Bioinorganic and Synthetic Chemistry / State Key Laboratory of Optoelectronic Materials and Technologies, School of Chemistry and Chemical Engineering, Sun Yat-Sen University,
Guangzhou 510275, P. R. China
Fax: +86-20-8411-2245
E-mail: tongml@mail.sysu.edu.cn

Supporting information for this article is available on the WWW under http://www.eurjic.org or from the author.

nuclear complexes of the same motif $[M\{Cu(dcadpz)_2\}M]^{4+}$.[15b] We speculated that a series of functional polydentate ligands may be designed and generated by introduction of other nucleophiles under different conditions, and that these ligands may be used in the synthesis of homo- and heterometallic clusters and metal-organic frameworks.[16]

In our continuing investigation of this interesting system, we report here the systematic preparation and characterization of a family of Cu^{II} complexes with five interesting ligands generated in situ by nucleophilic addition of MeOH and Hpz to dicyanamide under various conditions (Scheme 1). They are: $[Cu(HdcadMeOH)_2](ClO_4)_2{\cdot}2H_2O$ (**3**), $[Cu(dca)_2(3\text{-nic})_2]_n{\cdot}(HdcaMeOH)_{2n}$ (**4**), [Cu(dcapz)(dcadMeOH)] (**5**), $[Cu_3(dcadpz)_2(Hpz)_2(MeCN)_2](ClO_4)_2(NO_3)_2$ (**6**), and $[Cu_6(dcadpz\text{-}2H)_2(\mu\text{-}pz)_6]$ (**7**) [HdcadMeOH = bis(methoxycarbimido)amine; HdcaMeOH = (methoxycarbimido)cyanoamine; $dcapz^-$ = (pyrazolecarbimido)cyanoaminato; 3-nic = nicotinamide, which is occasionally introduced to the reaction system to trap the HdcaMeOH].

Results and Discussion

Synthesis and Characterization

Synthesis

Reaction temperature plays an important role in the nucleophilic addition reaction. In our case, all the complexes were obtained at 50–60 °C in 47–62% yields. The higher temperature may help to accelerate the nucleophilic attack since additional energy is needed for a coordinative activation of the β-carbon atom of the dca ligand changing its hybridization.[12] In fact, the [2+3] cycloaddition reaction of dicyanamide and azide ions was carried out under reflux or hydrothermal conditions in the presence of a Zn^{2+} or Cd^{2+} ion.[16]

Another important factor in relation to the product is the applied transition metal salts (if the reaction temperature was fixed at 50–60 °C). Both copper(II) perchlorate and copper nitrate can effectively mediate the nucleophilic addition reaction. It was previously documented that a zinc(II) salt was used to mediate similar reactions,[8–11] and that Ni^{II} salts have also been found to play the role of Cu^{II} in the synthesis of 1,3,5-triazapentadiene from nitrile and ammonia.[17] Moreover, the anions of the copper salts also play a vital role in the formation of the final products. If the synthesis of complex **3** was carried out by the replacement of copper(II) perchlorate by $Cu(BF_4)_2{\cdot}6H_2O$, a neutral complex $[Cu(dcadMeOH)_2]$[14] was obtained. Similar cases were also observed for the formation of complexes **4** and **5**. If another copper(II) salt was used in the synthesis of **6** and **7**, no crystal suitable for X-ray crystallography was obtained, indicating that the final products were dependent on the anions of the copper(II) salts, even though the anions did not coordinate with copper(II) ions.

Finally, it is noteworthy that the introduction of different silver(I) salts led to the formation of **6** and **7**, respectively. If no $AgNO_3$ is introduced into the reaction system, only the trinuclear complex $[Cu_3(dcadpz)_2(Hpz)_2(ClO_4)_2](ClO_4)_2{\cdot}H_2O$[14] can be obtained. However, hexanuclear complex **7** was formed if $AgNO_3$ was replaced by $AgBF_4$. The role of these silver salts cannot be ignored, though it is unclear to us at the moment.

The third notable factor is the effect of the molar ratio of dca^-/nucleophile on the product.[18] Theoretically, eight addition products of dca with nucleophiles of MeOH or Hpz can be expected (Scheme S1). When MeOH is used as the nucleophile, the 1:1 and 1:2 addition products can be expected (Scheme S1a–d). In fact, HdcaMeOH (Scheme S1b) was found in **4** in neutral form, $[dcadMeOH]^-$ (Scheme S1c) in **5** in deprotonated form, and HdcadMeOH (Scheme S1d) in **3** in neutral form. However, the 1:1 addition product of dca with MeOH (HdcaMeOH, Scheme S1b) in its deprotonated form ($dcaMeOH^-$, Scheme S1a) has not been trapped, which may be due to the presence of tautomerism of the protonated form (Scheme S1b). When Hpz is used as the nucleophile, the 1:1 and 1:2 addition products, $[dcapz]^-$ (Scheme S1e) and Hdcadpz, can be expected. Luckily, the addition product of Hdcadpz was trapped in $[dcadpz]^-$ form in **2** and **6** (Scheme S1f) and in $[dcadpz\text{-}2H]^{3-}$ form only in **7** (Scheme S1g). When the mixed nucleophiles of excess MeOH and less Hpz coexist in the reaction system, both $[dcadMeOH]^-$ and $[dcapz]^-$ were trapped as the addition

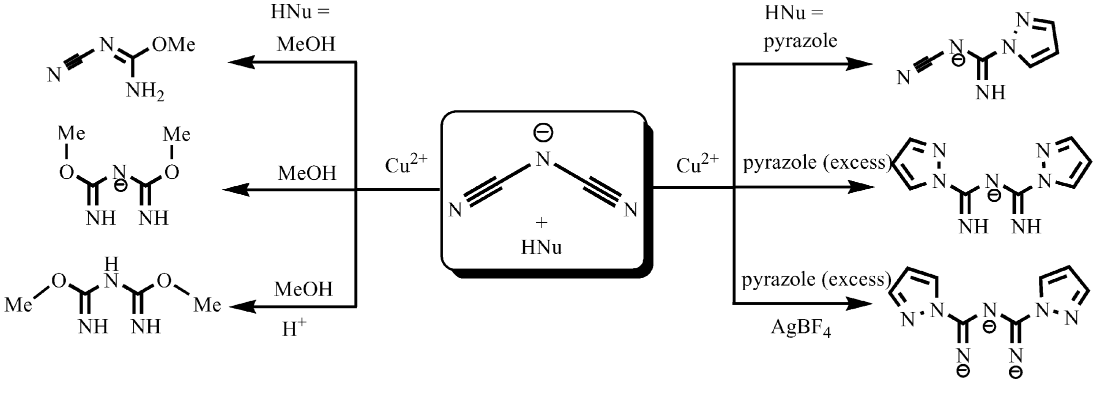

Scheme 1. Synthesis of **3**–**7**.

products in **5**. All addition products act as chelating ligands, except that in **4**. It should be noted that the Hdcadpz ligand generated in situ resembles the versatile multidentate cyclocarbophosphazene-containing ligand [{NP(3,5-Me_2Pz)$_2$}-{NC(3,5-Me_2Pz)}$_2$].[19]

Description of Crystal Structures

Crystal Structure of [Cu(HdcadMeOH)$_2$](ClO$_4$)$_2$·2H$_2$O (3)

The structure of **3** consists of $[Cu(HdcadMeOH)_2]^{2+}$ cations, ClO_4^- anions, and lattice water molecules. Selected bond lengths and angles are listed in Table 1. The Cu^{II} atom is coordinated in square-planar geometry by four nitrogen atoms from two neutral HdcadMeOH ligands (Figure 1a). The Cu1–N bond lengths are 1.951(3) and 1.955(3) Å, which are longer than the Cu–N bond lengths [1.939(2), 1.946(2) Å] in [Cu(dcadMeOH)$_2$].[14] The HdcadMeOH ligand apparently results from the 1:2 nucleophilic addition reaction of dca and MeOH (Scheme 1). The amide N2 atom was protonated in the presence of $HClO_4$. The two CH_3O groups of the HdcadMeOH ligand are in *syn*-*syn* conformation owing to the hydrogen atom bonded to the N2 atom, whereas in [Cu(dcadMeOH)$_2$] the two CH_3O groups of the [dcadMeOH]$^-$ ligand are in *anti*-*anti* conformation.[9,14] Similar conformational changes have been documented for the biguanide-like bidentate ligands in a variety of transition-metal complexes upon protonation/deprotonation, which alters their capacity to recognize complementary hydrogen-bonding motifs.[11a] Each Cu unit is further connected to two adjacent units through strong hydrogen bonding between the lattice water molecules and HdcaMeOH ligands [N2···O1w = 2.749(4) Å, N–H···O = 172(5)°], and an $R^2_4(8)$ hydrogen-bonded synthon [O1w···O3 = 2.913(1) Å] is formed between two H_2O molecules and two ClO_4^- anions, resulting in 1-D coordination chains (Figure 1b). These chains are further extended into 2D layers through the weak C–H···O hydrogen bonds (Figure S1).

Table 1. Selected bond lengths [Å] and angles [°] for **3**–**7**.[a]

3			
Cu(1)–N(3)	1.9484(18)	Cu(1)–N(1)	1.953(2)
N(3)–Cu(1)–N(1)	88.50(9)	N(3)–Cu(1)–N(1)	91.50(9)
4			
Cu(1)–N(1)	1.987(2)	Cu(1)–N(4)	2.0489(2)
Cu(1)–N(3b)	2.482(2)		
N(1)–Cu(1)–N(4)	88.27(8)	N(1)–Cu(1)–N(4a)	91.73(8)
N(1)–Cu(1)–N(3c)	87.30(8)	N(1)–Cu(1)–N(3b)	92.70(8)
N(4)–Cu(1)–N(3b)	89.97(7)	N(4)–Cu(1)–N(3c)	90.03(7)
5			
Cu(1)–N(1)	1.898(4)	Cu(1)–N(6)	1.966(3)
Cu(1)–N(2)	1.908(4)	Cu(1)–N(4)	2.005(4)
N(1)–Cu(1)–N(2)	90.31(16)	N(2)–Cu(1)–N(6)	176.16(17)
N(1)–Cu(1)–N(6)	93.39(16)	N(1)–Cu(1)–N(4)	172.94(15)
N(2)–Cu(1)–N(4)	96.53(16)	N(6)–Cu(1)–N(4)	79.74(14)
6			
Cu(1)–N(3)	1.956(4)	Cu(2)–N(5)	1.983(4)
Cu(1)–N(1)	1.962(3)	Cu(2)–N(7)	1.985(4)
Cu(2)–N(8)	1.954(4)	Cu(2)–N(10)	2.284(5)
Cu(2)–N(2)	1.958(3)		
N(3*a*)–Cu(1)–N(1)	91.07(14)	N(8)–Cu(2)–N(5)	99.56(15)
N(3)–Cu(1)–N(1)	88.93(14)	N(2)–Cu(2)–N(5)	80.20(14)
N(8)–Cu(2)–N(7)	98.43(16)	N(2)–Cu(2)–N(7)	79.82(14)
N(5)–Cu(2)–N(7)	157.30(16)	N(8)–Cu(2)–N(10)	95.20(18)
N(2)–Cu(2)–N(10)	94.01(17)	N(5)–Cu(2)–N(10)	97.87(19)
N(8)–Cu(2)–N(2)	170.73(16)		
7			
Cu(1)–N(3)	1.916(4)	Cu(2)–N(4)	1.984(4)
Cu(1)–N(1)	1.921(4)	Cu(2)–N(13a)	1.992(4)
Cu(1)–N(8)	2.011(4)	Cu(3)–N(3)	1.928(4)
Cu(1)–N(10)	2.058(4)	Cu(3)–N(11)	1.948(4)
Cu(2)–N(1)	1.942(4)	Cu(3)–N(12)	1.973(4)
Cu(2)–N(9)	1.960(4)	Cu(3)–N(6)	1.987(4)
N(3)–Cu(1)–N(1)	91.10(16)	N(9)–Cu(2)–N(13a)	93.87(16)
N(3)–Cu(1)–N(8)	172.20(17)	N(4)–Cu(2)–N(13a)	95.12(16)
N(1)–Cu(1)–N(8)	88.14(16)	N(3)–Cu(3)–N(11)	88.93(16)
N(3)–Cu(1)–N(10)	86.75(16)	N(3)–Cu(3)–N(12)	162.13(17)
N(1)–Cu(1)–N(10)	170.78(17)	N(11)–Cu(3)–N(12)	95.05(17)
N(8)–Cu(1)–N(10)	95.19(16)	N(3)–Cu(3)–N(6)	82.80(16)
N(1)–Cu(2)–N(9)	88.75(16)	N(11)–Cu(3)–N(6)	159.62(18)
N(1)–Cu(2)–N(4)	82.96(16)	N(12)–Cu(3)–N(6)	98.51(17)
N(9)–Cu(2)–N(4)	170.80(16)	Cu(1)–N(1)–Cu(2)	121.3(2)
N(1)–Cu(2)–N(13a)	166.41(17)	Cu(1)–N(3)–Cu(3)	120.8(2)

[a] Symmetry codes for **3**: (a) $-x + 1$, $-y - 1$, $-z$; (b) x, $-y - 1$, z; for **4**: (a) $-x + 1$, $-y + 1$, $-z + 1$; (b) x, $y - 1$, z; (c) $-x + 1$, $-y + 2$, $-z + 1$; (d) x, $y + 1$, z; for **6**: (a) $-x - 2$, $-y$, $-z$; for **7**: (a) $-x$, $-y + 1$, $-z + 1$.

Crystal Structure of [Cu(dca)$_2$(3-nic)$_2$]$_n$·(HdcaMeOH)$_{2n}$ (4)

Complex **4** consists of 1-D neutral coordination chains formulated with [Cu(dca)$_2$(3-nic)$_2$]$_n$ and a new 1:1 addition product of dca with MeOH. These 1D chains are of the type commonly found in coordination chemistry of the dca$^-$ ligand.[6] The copper atom is coordinated in [4+2] CuN_6 octahedral geometry to four $\mu_{1,5}$-dca$^-$ anions, coordinating through the nitrile nitrogen atoms [Cu1–N_{dca} 1.987(2) and 2.482(2) Å], and two *trans*-related 3-nic ligands, coordinating through the pyridyl nitrogen donors [Cu1–N_{3-nic} = 2.0489(2) Å], as depicted in Figure 2a. The *cis*-N–Cu1–N bond angles deviate only slightly from O_h symmetry and range from 87.30(8) to 92.70(8)°. As documented in the reported dca-bridged complexes,[6] the dca anions do not coordinate linearly to the metal center with C–N–Cu1 angles of 145.6(2) and 159.6(2)°. The Cu^{II} atoms are doubly connected by $\mu_{1,5}$-dca bridges into 1-D linear chains with the shortest intrachain and interchain Cu···Cu separations of 7.058(5) and 7.572(5) Å, respectively.

It should be noted that a new 1:1 addition product of MeOH to dca, N≡C–N=C(MeO)–NH_2 (HdcaMeOH, Scheme 1), is trapped in **4**. The IR peak at 1660 cm^{-1} provides evidence of the existence of the N=C group, and the peak at 2228 cm^{-1} proves the existence of the N≡C group. Different from those in other complexes, the addition product HdcaMeOH in **4** acts as the guest molecule, which may be contributed to the synergic interactions between host chains and guest molecules. 2-D hydrogen-bonded supramolecular thick double-layers are formed with the 1-D coordination chains (Figure 2b) and the encapsulated HdcaMeOH guests through the N–H···$N_{nitrile}$ and N–H···

© 2008 Wiley-VCH Verlag GmbH & Co. KGaA, Weinheim

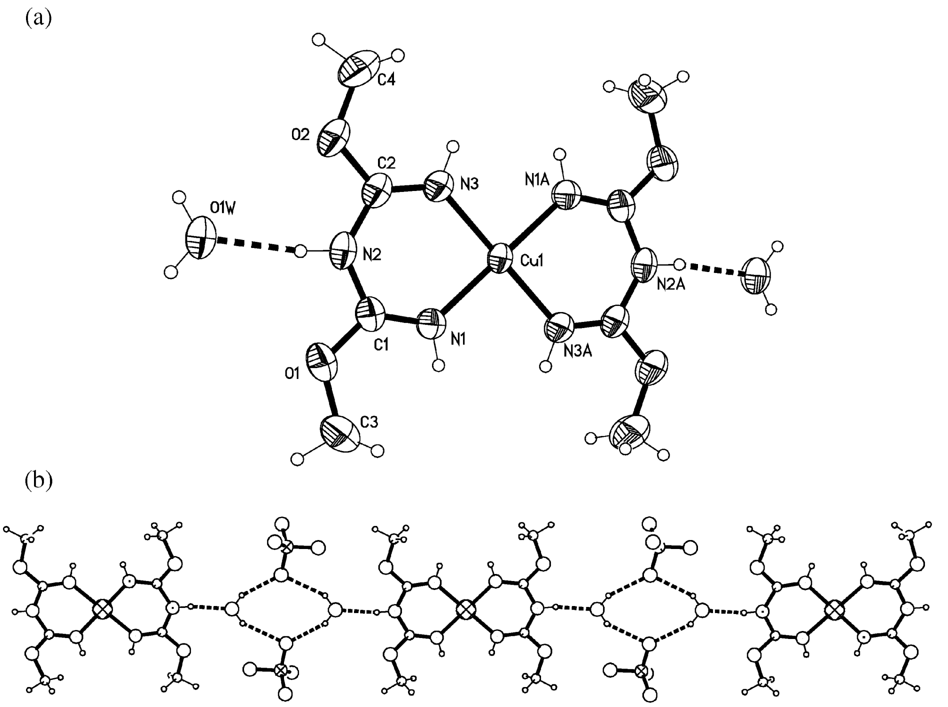

Figure 1. Perspective views of the coordination environment of the Cu^{II} ion (a) and the 1-D hydrogen-bonded chain (b) in **3**.

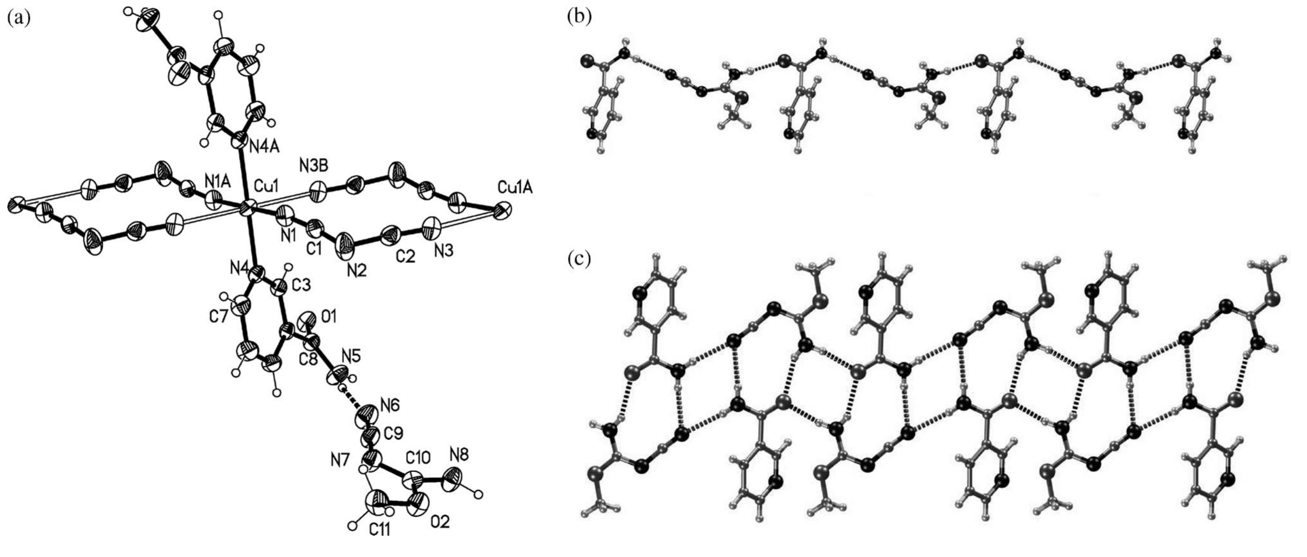

Figure 2. Perspective views of the coordination environment of the Cu^{II} ion (a), the 1-D hydrogen-bonded [HdcaMeOH·(3-nic)] chain (b), and the interlayer self-complementary hydrogen-bonding interactions (c) in **4**.

$O_{carbonyl}$ hydrogen bonds between HdcaMeOH and the terminal 3-nic ligands (Figure 2c). Adjacent 2D layers are further extended into a 3-D hydrogen-bonded network (Figure S2a) through interlayer self-complementary N–H···$N_{nitrile}$ and N–H···$O_{carbonyl}$ hydrogen bonds (Figure S2b). Three supramolecular synthons of $R^2_2(10)$, $R^2_4(8)$, and $R^2_4(6)$ patterns are formed among two HdcaMeOH molecules and two 3-nic motifs [N–H···O 2.878(1) Å, N–H···O 151.1(2)°; N–H···N 3.074(1) Å, N–H···N 170.4(4)°; N–H···N 3.074(1) Å, 3.102(1) Å, N–H···N 170.4(4)°, 152.1(6)°; N–H···N 2.942(2) Å, 2.956(2) Å, N–H···O 170.0(1)° and 151.1(2)°]. In addition, a weak C–H···N hydrogen bond[20] between 3-nic and dca motifs exists within the 3-D supramolecular network.

Crystal Structure of [Cu(dcapz)(dcadMeOH)] (5)

Complex **5** is a neutral planar Cu^{II} complex (Figure 3a). The Cu^{II} atom is coordinated in a square-planar geometry to four nitrogen atoms from one $[dcadMeOH]^-$ ligand and one $dcapz^-$ ligand, the Cu1–N bond lengths are 1.894(4)–2.005(4) Å. The two CH_3O groups are in *anti-anti* conformation. The $[dcadMeOH]^-$ ligand is apparently formed by

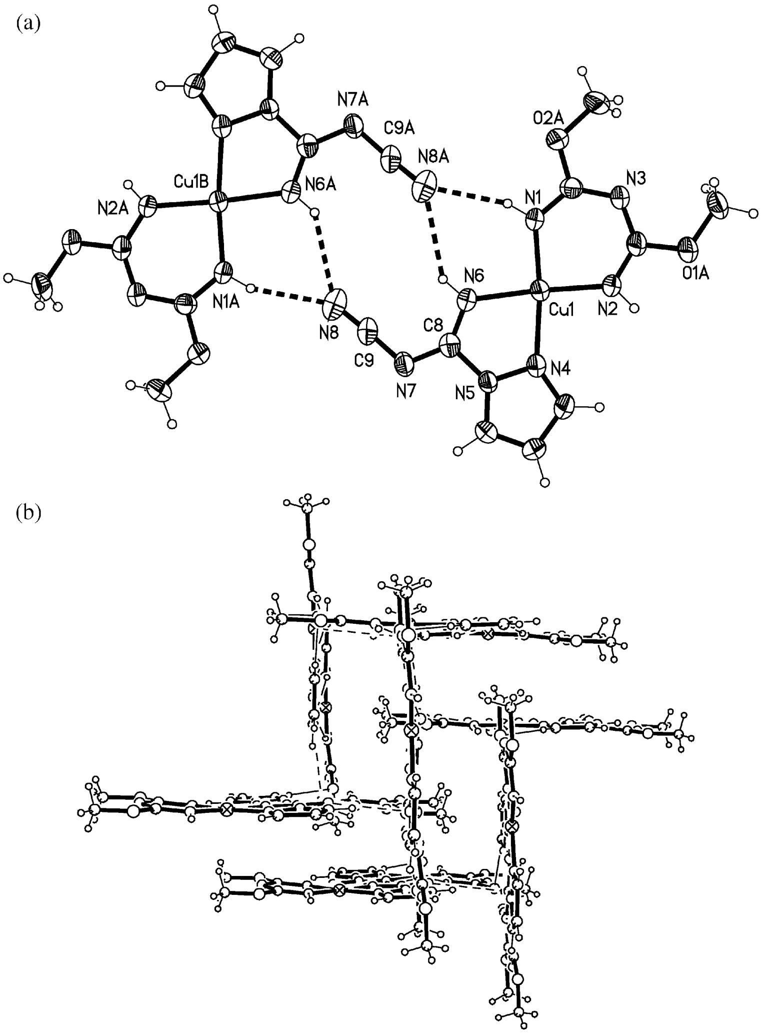

Figure 3. Perspective views of the coordination environment of the Cu^{II} ion and the hydrogen-bonded dimer (a) and the hydrogen-bonded synthon of one dimeric motif with four neighboring dimers (b) in **5**.

a 1:2 nucleophilic addition of MeOH to dca, which can also be found in $[Cu(dcadMeOH)_2]$,[14] and the $[dcapz]^-$ ligand results from the 1:1 nucleophilic addition of Hpz to dca, as shown in Scheme 1. The $[dcapz]^-$ ligand was previously trapped in a mononuclear $[Ni(dcapz)_2]$.[18c] A pair of neighboring mononuclear species are linked by intermolecular self-complementary N_{imido}–H···N_{cyano} hydrogen bonds between the cyano and amino groups [N1···N6a 3.109(6), N4···N6a 3.249(6) Å; N1–H1N···N6a 160(3), N4–H4N···N6a 139(3)°], which is displayed in Figure 3a. Each dimeric motif is further connected by four neighboring motifs (Figure 3b) through N–H···O and C–H···O hydrogen bonds into a 3-D hydrogen-bonded network (Figure S3).

Crystal Structure of $[Cu_3(dcadpz)_2(Hpz)_2(MeCN)_2](ClO_4)_2(NO_3)_2$ *(6)*

Similar to **1**, **6** is a symmetrical linear trinuclear copper(II) complex, as illustrated in Figure 4. The crystallographically asymmetric unit consists of one half of a formula unit, and therefore, there are 1.5 Cu^{II} centers, one $dcadpz^-$, one Hpz, and one MeCN ligand as well as one ClO_4^- and one NO_3^- anion. The $dcadpz^-$ ligand apparently results from the addition of Hpz to dca in a 2:1 molar ratio (Scheme 1), which was also found in **1**. The central Cu1 atom is located at an inversion center and is coordinated in a perfectly square-planar geometry to four nitrogen atoms from two $dcadpz^-$ ligands, with Cu1–N bond lengths of 1.956(7) and 1.962(7) Å, longer than those found in **2**

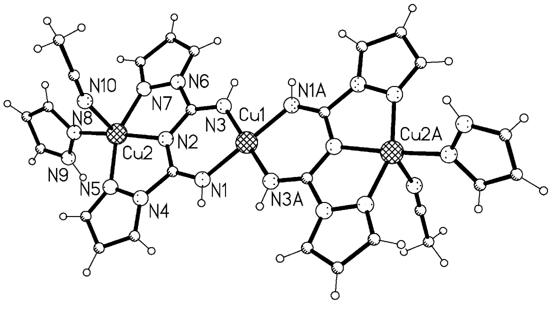

Figure 4. Perspective view of the coordination environment of the Cu^{II} ions in **6**.

© 2008 Wiley-VCH Verlag GmbH & Co. KGaA, Weinheim

[1.949(4), 1.955(4) Å]. Each of the terminal Cu2 atoms is coordinated in a tetragonal-pyramidal geometry with three nitrogen atoms from a $dcadpz^-$ ligand [Cu2–N 1.958(4)–1.985(7) Å] and one Hpz ligand [Cu2–N8 1.954(7) Å] in the equatorial positions and one acetonitrile ligand in the apical position [Cu2–N10 2.284(7) Å]. Neighboring Cu3 units are further linked by NO_3^- groups into a 1-D hydrogen-bonded chain structure through a weak C–H···O hydrogen-bonding interaction [C4···O3 3.391(3), C6···O3 3.196(2) Å].

Crystal Structure of [Cu_6(dcadpz-2H)$_2$(μ-pz)$_6$] (7)

Complex **7** is a neutral hexanuclear copper(II) ring consisting of six Cu^{II} ions, two $[dcadpz\text{-}2H]^{3-}$ ligands, and six pz^- ligands. Different from that trapped in complexes **1** and **6**, each Hdcadpz ligand in **7** is in $[dcadpz\text{-}2H]^{3-}$ form with all coordinated imine and pyrazolyl N atoms oriented along one side and acting in a $\mu_3{:}\eta^1{:}\eta^2{:}\eta^2{:}\eta^1$ bridging mode to link three Cu^{II} centers arranged almost in a linear array to form the $[Cu_3(dcadpz\text{-}2H)]^{3+}$ motif. Within $[Cu_3(dcadpz\text{-}2H)]^{3+}$, the three Cu^{II} ions are also bridged by two μ-pz^- ligands. A pair of the thus-formed $[Cu_3(dcadpz\text{-}2H)(pz)_2]^+$ subunits are linked into a circle by two μ-pz^- ligands (Figure 5). All the copper(II) ions are in a square-planar coordination geometry. The central Cu1 atom is coordinated to two chelated imine nitrogen atoms from one $[dcadpz\text{-}2H]^{3-}$ ligand and two pz^- ligands. The Cu1–N bond lengths are 1.915(1)–2.058(1) Å. Each of the Cu2 and Cu3 atoms is also coordinated to two nitrogen atoms from a $[dcadpz\text{-}2H]^{3-}$ ligand and two pz^- ligands. The Cu2–N bond lengths are 1.942(1)–1.993(1) Å. The intracircle Cu1···Cu2 and Cu2···Cu3 distances are 3.342(2) Å and 3.367(2) Å, respectively, the intracircle Cu2···Cu3a and Cu2a···Cu3 distances separated by unique pz^- bridges are 3.210(3) Å. The Cu_6 cluster rings stack with each other into 2D layers, as shown in Figure S4.

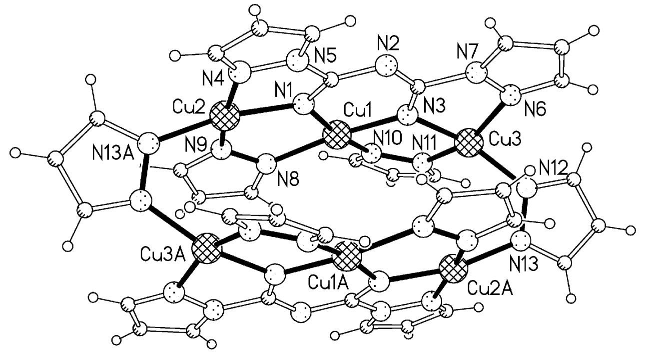

Figure 5. Perspective view of the coordination environment of the Cu^{II} ions in **7**.

Magnetic Properties of 6 and 7

The dc magnetic properties of **6** in the form of $\chi_M T$ vs. T plots (χ_M is the magnetic susceptibility per trinuclear unit) are shown in Figure 6a. The $\chi_M T$ value at room temperature is 1.26 $cm^3 mol^{-1}$ K, slightly larger than that for three uncoupled unpaired electrons (0.375 × 3, assuming g = 2.00). Upon lowering the temperature, $\chi_M T$ gradually increases from 1.26 $cm^3 mol^{-1}$ K at 305 K to reach a maximum of 2.00 $cm^3 mol^{-1}$ K at 2.5 K and then decreases to 1.98 $cm^3 mol^{-1}$ K at 2 K. The $1/\chi_m$ vs. T plot (300–2 K) obeys the Curie–Weiss law with C = 1.25 $cm^3 mol^{-1}$ K, θ = 3.59 K. The C value corresponds to g = 2.10. The successive increase of χ_m and positive θ value suggest the operation of a ferromagnetic coupling interaction between the three S = 1/2 spins within the Cu_3 cluster through the $dcadpz^-$ bridges. The temperature dependence of $\chi_M T$ was analyzed by an isolated three-spin mode[21,22] [$H = -2J(S_{Cu2}\cdot S_{Cu1} + S_{Cu1}S_{Cu2'})$] with MAGMUN4.1.[23] The best-fit parameters obtained with this computing model are J = 6.91 cm^{-1}, zJ' = –0.016 cm^{-1}, g_{av} = 2.09, $R = 1.01 \times 10^{-4}$ {$R = [\Sigma(\chi_{obs} - \chi_{calc})^2/\Sigma\chi_{obs}{}^2]^{1/2}$}. These fitting results reveal that $Cu(dcadpz)_2$ is ferromagnetically coupled with both the terminal Cu^{II} ions and therefore each Cu–Cu–Cu unit has a ground spin multiplicity of 3/2. The reduced molar magnetization ($M/N\beta$) per Cu_3 unit in the range 0–70 kOe at 2 K is shown in Figure 6b. The experimental curve gradually approaches the theoretical curve (solid line in Figure 6b) of M/H for the S = 3/2 state (g = 2.09). The ferromagnetic

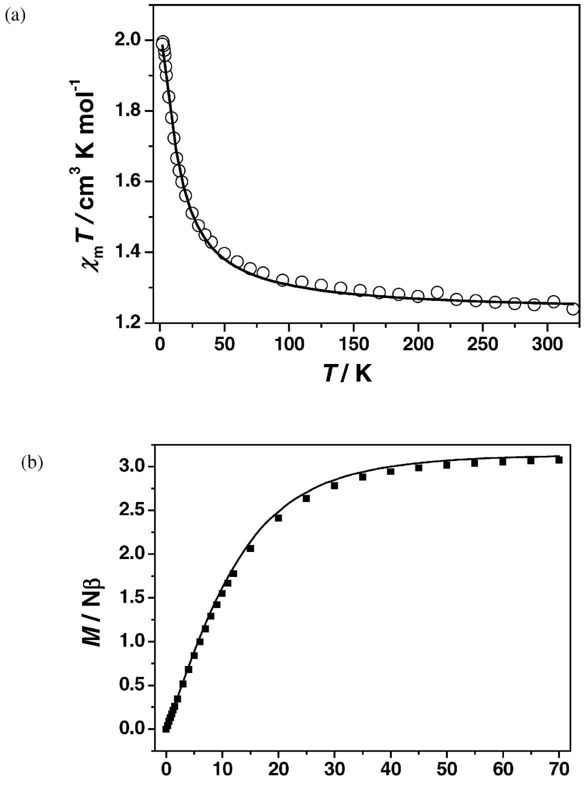

Figure 6. (a) Plot of $\chi_M T$ vs. T. The solid line represents the best fit with the parameters given in the text for **6**. (b) The field dependence of the magnetization measured at 2 K for **6**. The solid lines represent the theoretical curve per trinuclear unit calculated with the Brillouin functions.

interaction apparently results from the orthogonality of the symmetric magnetic orbitals of the terminal Cu^{II} ions and antisymmetric magnetic orbital of the central Cu^{II} ion. In complex **6**, the $Cu_{central}$ atom is antisymmetric, whereas the $Cu_{terminal}$ atom is symmetric, and hence, the magnetic orbitals are orthogonal to each other, similar to those found in previously reported linear Cu^{II}–Cu^{II}–Cu^{II} systems.[14,15]

The magnetic property of complex **7** in the form of the χ_M vs. T plot (χ_M is the molar magnetic susceptibility for six Cu^{II} ions) is shown in Figure 7. The $\chi_M T$ curve (Figure S5) starts at ca. 1.36 $cm^3 mol^{-1} K$, lower than the value for six uncoupled unpaired electrons (0.375×6, assuming $g = 2.00$). From room temperature down to 2 K, the $\chi_M T$ product decreases continuously to 0.49 $cm^3 mol^{-1} K$ at 2 K, which is indicative of strong antiferromagnetic coupling within the Cu_6 cluster through the pz^- and $[dcadpz\text{-}2H]^{3-}$ bridges. Considering cluster topology and connectivity, the exchange pathway in **7** is shown in Figure 7b. The temperature dependence of χ_M was analyzed on the basis of a theoretical expression[24] derived from a spin Hamiltonian [$H = -J_2(S_1\cdot S_2 + S_2\cdot S_3 + S_4\cdot S_5 + S_5\cdot S_6) - J_1(S_3\cdot S_4 + S_6\cdot S_1)$] including the temperature-independent paramagnetism (*TIP*). The best-fit parameters obtained are: $g = 2.10$, $2J_1/k_B = -69.1$ K, $2J_2/k_B = -250.6$ K and $TIP = 4 \times 10^{-4}$ $cm^3 mol^{-1}$ (fixed), $R = 1.02 \times 10^{-5}$ {$R = [\Sigma(\chi_{obs} - \chi_{calc})^2/\Sigma\chi_{obs}^2]^{1/2}$}. The fitting results are consistent with the structural features of **7** since there are two kinds of magnetic exchange pathways (one is composed of both the single-atom bridge and pz^- bridge and another consists of the unique pz^- ligand).[25,26]

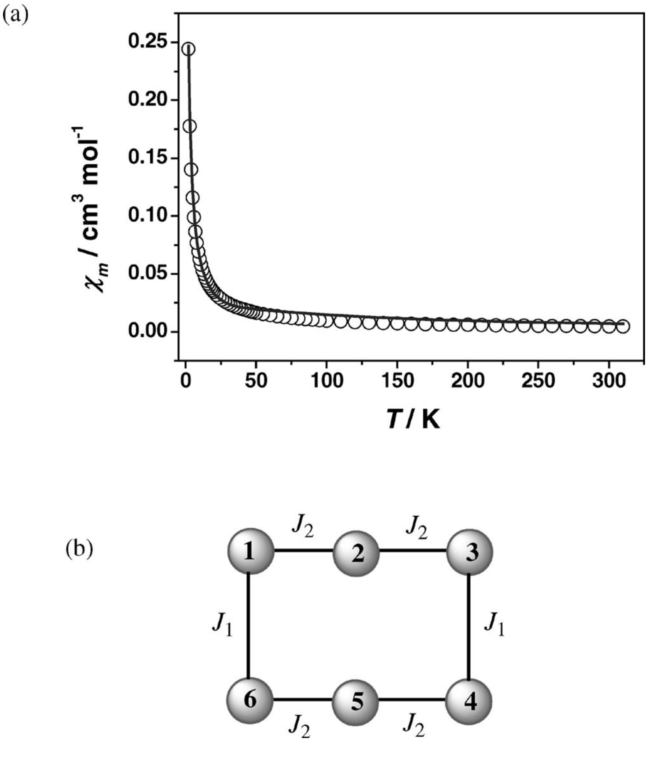

Figure 7. (a) Plot of χ_M vs. T. The solid line represents the best fit with the parameters given in the text for **7**. (b) Schematic diagrams representing the exchange interactions within **7**.

Conclusions

In this work, Cu^{II}-mediated in-situ nucleophilic additions of nucleophiles (MeOH, Hpz) to dicyanamide in different molar ratios were carried out, from which five new mononuclear, trinuclear, hexanuclear and one-dimensional copper(II) complexes **3**–**7** were obtained. Meanwhile, the unique 1:1 addition product HdcaMeOH and a new coordination mode of the polydentate dcadpzH ligand, $[dcadpz\text{-}2H]^{3-}$, were trapped in **4** and **7**, respectively. Magnetic studies revealed that ferromagnetic and antiferromagnetic interactions exist in **6** and **7**, respectively, as a result of the polydentate Hdcadpz ligand in different coordination modes, which provides a new route to magnetic homo- and heterotrinuclear clusters.

Experimental Section

General: All chemicals were used as purchased from commercial vendors without further purification. The C, H, and N microanalyses were carried out with an Elementar Vario-EL CHNS elemental analyzer. The FT-IR spectra were recorded from KBr pellets in the range 4000–400 cm^{-1} with a Bio-Rad FTS-7 spectrometer. The variable-temperature magnetic-susceptibility data were measured with a Quantum Design MPMS7 SQUID magnetometer. Magnetic measurements were performed on samples of crushed single crystals in the 2–300 K range. Diamagnetic corrections were made with Pascal's constants.

CAUTION! Metal perchlorates containing organic ligands are potentially explosive. Only a small amount of material should be prepared and handled with great care.

Synthesis of $[Cu(HdcadMeOH)_2](ClO_4)_2\cdot 2H_2O$ (3): Sodium dicyanamide (0.045 g, 0.5 mmol) was dissolved in a CH_3OH/H_2O (5:1, v/v) mixture (30 mL). To this solution was added a dilute aqueous solution (10 mL) of $Cu(ClO_4)_2\cdot 6H_2O$ (0.094 g, 0.25 mmol) whilst stirring at 50 °C, and a small amount of blue precipitate was observed. Dilute $HClO_4$ (0.5 mmol) was added. The resultant solution was filtered and left to stand at room temperature. Purple block crystals suitable for X-ray diffraction were obtained by slow evaporation of the solvents within one week. Yield: 0.070 g, 50% based on Cu. $C_8H_{22}Cl_2CuN_6O_{14}$ (560.76): calcd. C 17.14, H 3.95, N 14.99; found C 17.30, H 4.04, N 14.90. IR (KBr): $\tilde{\nu}$ = 3601 (m), 3523 (m), 3373 (s), 3297 (w), 3249 (w), 3048 (w), 2960 (w), 2913 (w), 2582 (w), 2024 (w), 1677 (vs), 1595 (s), 1468 (m), 1405 (vs), 1235 (s), 1186 (w), 1143 (m), 1090 (m), 1001 (w), 921 (m), 761 (s), 689 (m), 671 (s), 485 (m) cm^{-1}.

Synthesis of $[Cu(dca)_2(3\text{-}nic)_2]_n\cdot(HdcaMeOH)_{2n}$ (4): A methanol solution (10 mL) of $Cu(NO_3)_2\cdot 3H_2O$ (0.121 g, 0.5 mmol) was added dropwise to a CH_3OH/H_2O (5:1, v/v) solution (20 mL) containing sodium dicyanamide (0.134 g, 1.5 mmol) and 3-nic (0.122 g, 1.0 mmol) under vigorous stirring. The mixture was heated with stirring at 60 °C for ca. 30 min and then filtered after cooling to room temperature. Well-shaped blue-purple block crystals of **4** suitable for X-ray diffraction were obtained within one week upon slow evaporation of the solvents. Yield: 0.128 g, 40% based on Cu. $C_{22}H_{22}CuN_{16}O_4$ (638.10): calcd. C 41.41, H 3.48, N 35.12; found C 41.39, H 3.40, N 35.08. IR (KBr): $\tilde{\nu}$ = 3591 (w), 3404 (m), 3327 (m), 3239 (vw), 3169 (m), 2951 (w), 2442 (vw), 2301 (s), 2228 (s), 2173 (vs), 1660 (vs), 1619 (m), 1579 (s), 1487 (s), 1447 (m), 1392 (m), 1097 (m), 998 (m), 939 (w), 823 (w), 697 (m), 517 (w) cm^{-1}.

© 2008 Wiley-VCH Verlag GmbH & Co. KGaA, Weinheim

Table 2. Crystallographic data and structure-refinement parameters for **3**–**7**.

	3	**4**	**5**	**6**	**7**
Empiorical formula	$C_8H_{22}Cl_2CuN_6O_{14}$	$C_{22}H_{22}CuN_{16}O_4$	$C_9H_{12}CuN_8O_2$	$C_{26}H_{30}Cl_2Cu_3N_{22}O_{14}$	$C_{34}H_{30}Cu_6N_{26}$
Formula mass	560.76	638.10	327.81	1136.24	1184.08
Cryst system	monoclinic	triclinic	monoclinic	triclinic	triclinic
Space group	$C2/m$ (No. 12)	$P\bar{1}$ (No. 2)	$P2_1/n$ (No. 14)	$P\bar{1}$ (No. 2)	$P\bar{1}$ (No. 2)
a [Å]	16.848(3)	7.0589(9)	11.350(2)	7.2977(9)	8.256(1)
b [Å]	6.2217(9)	7.573(1)	9.799(1)	11.448(1)	11.233(1)
c [Å]	10.6653(16)	13.062(2)	11.755(2)	12.869(2)	11.996(2)
α [°]	90	91.035(2)	90	89.585(2)	106.433(2)
β [°]	109.049(2)	105.557(2)	100.462(2)	81.385(2)	92.944(2)
γ [°]	90	96.258(2)	90	87.035(2)	105.936(2)
V [Å^3]	1056.8(3)	667.8(2)	1285.7(3)	1061.6(2)	1016.0(2)
Z	1	1	4	1	1
$D_{\text{calcd.}}$ [g cm^{-3}]	1.762	1.587	1.694	1.777	1.935
T [K]	293(2)	293(2)	293(2)	293(2)	293(2)
λ (Mo-K_α) [Å]	0.71073	0.71073	0.71073	0.71073	0.71073
μ [mm^{-1}]	1.365	0.882	1.715	1.705	3.149
R_1 [$I > 2\sigma(I)$][a]	0.0402	0.0423	0.0553	0.0484	0.0446
wR_2 [$I > 2\sigma(I)$][b]	0.1132	0.1053	0.1232	0.1343	0.1017
R_1 (all data)[a]	0.0431	0.0460	0.0737	0.0581	0.0622
wR_2 (all data)[b]	0.1152	0.1080	0.1324	0.1434	0.1104

[a] $R_1 = \Sigma||F_o| - |F_c||/\Sigma|F_o|$. [b] $wR_2 = [\Sigma w(|F_o| - |F_c|)^2/\Sigma w|F_o|^2]^{1/2}$.

Synthesis of [Cu(dcapz)(dcadMeOH)] (5): Pyrazole (0.034 g, 0.5 mmol) and sodium dicyanamide (0.089 g, 1.0 mmol) were mixed in a CH_3OH/H_2O (5:1, v/v) solution (20 mL), to which an aqueous solution (8 mL) of $Cu(NO_3)_2 \cdot 3H_2O$ (0.120 g, 0.5 mmol) was slowly added with vigorous stirring at 60 °C. A small amount of blue precipitate was formed which was then dissolved by adding additional water (10 mL). The blue filtrate was allowed to stand at room temperature, and blue-purple block single crystals suitable for X-ray diffraction were obtained by evaporation of the solvents within one week. Yield: 0.107 g, 65%. $C_9H_{12}CuN_8O_2$ (327.81): calcd. C 32.98, H 3.69, N 34.18; found C 32.43, H 4.67, N 30.77. IR (KBr): ṽ = 3440 (w), 3334 (m), 3123 (m), 2993 (w), 2954 (w), 2847 (w), 2418 (w), 2308 (w), 2253 (w), 2171 (vs), 1603 (vs), 1471 (s), 1378 (s), 1251 (m), 1198 (m), 1153 (m), 1088 (m), 1051 (s), 972 (w), 822 (w), 791 (w), 739 (m), 579 (m), 470 (w) cm^{-1}.

Synthesis of $[Cu_3(dcadpz)_2(Hpz)_2(MeCN)_2](ClO_4)_2(NO_3)_2$ (6): A methanol solution (10 mL) of $Cu(ClO_4)_2 \cdot 6H_2O$ (0.555 g, 1.5 mmol) was added dropwise to a CH_3OH/H_2O (5:1, v/v) solution (20 mL) containing sodium dicyanamide (0.089 g, 1.0 mmol) and pyrazole (0.204 g, 3.0 mmol) under vigorous stirring. A blue solution formed on addition of metal salt to the ligands. The mixture was heated with stirring at 60 °C for ca. 30 min and then an acetonitrile solution (5 mL) of $AgNO_3$ (0.085 g, 0.5 mmol) was added; the solution turned to deep blue, and some precipitate was soon formed. The mixture was filtered after cooling to room temperature. Well-shaped blue block crystals of **6** suitable for X-ray diffraction were obtained within one week upon slow evaporation of the solvents. Yield: 0.284 g, 50%. $C_{26}H_{30}Cl_2Cu_3N_{22}O_{14}$ (1136.24): calcd. C 27.48, H 2.66, N 27.12; found C 27.45, H 2.65, N 27.09. IR (KBr): ṽ = 3217 (m), 3134 (m), 3086 (w), 2018 (vw), 16661 (vs), 1607 (m), 1529 (w), 1462 (m), 1403 (s), 1346 (m), 1297 (s), 1230 (w), 1107 (m), 1065 (m), 981 (m), 913 (w), 828 (w), 776 (m), 726 (m), 624 (s), 452 (vw) cm^{-1}.

Synthesis of $[Cu_6(dcadpz\text{-}2H)_2(\mu\text{-}pz)_6]$ (7): A methanol solution (10 mL) of $Cu(ClO_4)_2 \cdot 6H_2O$ (0.277 g, 0.75 mmol) was added dropwise to a CH_3OH/H_2O (5:1, v/v) solution (20 mL) containing sodium dicyanamide (0.089 g, 1.0 mmol) and pyrazole (0.136 g, 2.0 mmol) under vigorous stirring. A blue solution formed on addition of metal salt to the ligands. The mixture was heated with stirring at 60 °C for ca. 30 min, and then an acetonitrile solution (5 mL) of $AgBF_4$ (0.146 g, 0.75 mmol) was added, the solution turned dark green, and some precipitate was soon formed. The mixture was filtered after cooling to room temperature. Needle-shaped dark green crystals of **7** suitable for X-ray diffraction were obtained within one week. Yield: 0.053 g, 36% based on copper salt. $C_{34}H_{30}Cu_6N_{26}$ (1184.08): calcd. C 34.49, H 2.55, N 30.76; found C 34.38, H 2.64, N 30.56. IR (KBr): ṽ = 3419 (vw), 3148 (m), 2922 (m), 2851 (w), 1744 (w), 1660 (w), 1599 (s), 1515 (m), 1488 (m), 1433 (w), 1382 (m), 1349 (s), 1325 (m), 1301 (m), 1253 (w), 1202 (m), 1175 (w), 1049 (vs), 991 (w), 943 (m), 876 (w), 809 (s), 756 (vs), 676 (w), 627 (s), 582 (m) cm^{-1}.

X-ray Crystallographic Study: The data collections were carried out with a Bruker SMART Apex CCD diffractometer by using graphite-monochromated Mo-K_α radiation (λ = 0.71073 Å) at 293 K (frames of 0.3° oscillation). Absorption corrections were applied by using SADABS.[27] The structures were solved with direct methods and refined with a full-matrix least-squares technique with the SHELXTL package.[28] Anisotropic thermal parameters were applied to all non-hydrogen atoms. The organic hydrogen atoms were generated geometrically, the aqua hydrogen atoms were located from difference maps and refined with isotropic temperature factors. The crystallographic data for **3**–**7** are summarized in Table 2. CCDC-688303 (**3**), -688304 (**4**), -688305 (**5**), -688306 (**6**), and -688307 (**7**) contain the supplementary crystallographic data for this paper. These data can be obtained free of charge from The Cambridge Crystallographic Data Centre via www.ccdc.cam.ac.uk/data_request/cif.

Supporting Information (see footnote on the first page of this article): Products generated in situ by nucleophilic additions of different nucleophiles to dicyanamine in complexes **3**–**7**; hydrogen-bonded layers or networks in **3**, **4**, **5**, and **7**.

Acknowledgments

This work was supported by the National Natural Science Foundation of China (20525102), the Research Fund for the Doctoral Program of Higher Education (20060558081), and the National Basic Research Program of China (2007CB815305).

[1] a) B. N. Storhoff, H. C. Lewis, *Coord. Chem. Rev.* **1977**, *23*, 1–29; b) B. Corain, M. Basato, A. C. Veronese, *J. Mol. Catal.* **1993**, *81*, 133–155; c) X.-M. Chen, M.-L. Tong, *Acc. Chem. Res.* **2007**, *40*, 162–170; d) X.-M. Zhang, *Coord. Chem. Rev.* **2005**, *249*, 1201–1219; e) H. Zhao, Z.-R. Qu, H.-Y. Ye, R.-G. Xiong, *Chem. Soc. Rev.* **2008**, *37*, 84–100.

[2] a) A. G. Sharpe, *The Chemistry of Cyano Complexes of the Transition Metals*, Academic Press, London, **1976**; b) R. W. Hay in *Reactions of Coordinated Ligands* (Ed.: P. S. Braterman), Plenum Press, New York, **1989**, vol. 2, p. 280; c) E. C. Constable, *Metals and Ligand Reactivity – An Introduction to the Organic Chemistry*, VCH, Weinheim, **1995**, p. 65.

[3] a) V. Y. Kukushkin, A. J. L. Pombeiro, *Chem. Rev.* **2002**, *102*, 1771–1802; b) A. J. L. Pombeiro, V. Y. Kukushkin, "Reactions of Coordinated Nitriles" in *Comprehensive Coordination Chemistry* (Eds.: J. A. McCleverty, T. J. Meyer), 2nd ed., Elsevier, Oxford, UK, **2003**, vol. 1, p. 639; c) R. A. Michelin, M. Mozzon, R. Bertani, *Coord. Chem. Rev.* **1996**, *147*, 299–338; d) J.-R. Li, Y. Tao, Q. Yu, X.-H. Bu, *Chem. Commun.* **2007**, 1527–1529.

[4] J. Eglin, *Comments Inorg. Chem.* **2002**, *23*, 231–238.

[5] a) M. N. Kopylovich, V. Y. Kukushkin, M. F. C. Guedes da Silva, M. Haukka, J. J. R. Fraústo da Silva, A. J. L. Pombeiro, *J. Chem. Soc. Perkin Trans. 1* **2001**, 1569–1573; b) J. Burgess, C. D. Hubbard, *Adv. Inorg. Chem.* **2003**, *54*, 71–155; c) V. Y. Kukushkin, A. J. L. Pombeiro, *Inorg. Chim. Acta* **2005**, *358*, 1–21.

[6] See reviews: a) S. R. Batten, K. S. Murray, *Coord. Chem. Rev.* **2003**, *246*, 103–130; b) X.-Y. Wang, Z.-M. Wang, S. Gao, *Chem. Commun.* **2008**, 281–294.

[7] W. P. Norris, R. A. Henry, *J. Org. Chem.* **1964**, *29*, 650–660.

[8] J. Kozisek, M. Hvastijova, J. Kohout, *Inorg. Chim. Acta* **1990**, *168*, 157–158.

[9] R. Boča, M. Hvastijova, J. Kozisek, M. Valko, *Inorg. Chem.* **1996**, *35*, 4794–4797.

[10] M. B. Michael, F. L. Leonard, M. Srihari, T. Peter, *J. Chem. Soc., Dalton Trans.* **2000**, 233–234.

[11] a) I. M. Atkinson, M. M. Bishop, F. L. Leonard, M. Srihari, T. Peter, *Chem. Commun.* **2002**, 2818–2819; b) X.-H. Zhao, X.-D. Chen, M. Du, *Acta Crystallogr., Sect. E* **2006**, *62*, m3580–m3581; c) G.-F. Liu, L.-L. Li, Y. Zhang, J.-P. Lang, S. W. Ng, *Acta Crystallogr., Sect. C* **2007**, *63*, m1–m3.

[12] M. Hvastijová, J. Kohout, J. Buchler, W. Boča, J. Kožíšek, L. Jäger, *Coord. Chem. Rev.* **1998**, *175*, 17–42.

[13] M.-L. Tong, J. Ru, Y.-M. Wu, X.-M. Chen, H.-C. Chang, K. Mochizuki, S. Kitagawa, *New J. Chem.* **2003**, *27*, 779–782.

[14] M.-L. Tong, Y.-M. Wu, Y.-X. Tong, X.-M. Chen, H.-C. Chang, S. Kitagawa, *Eur. J. Inorg. Chem.* **2003**, 2385–2388.

[15] a) L.-L. Zheng, W.-X. Zhang, L.-J. Qin, J.-D. Leng, J.-X. Lu, M.-L. Tong, *Inorg. Chem.* **2007**, *46*, 9548–9557; b) A. Igashira-Kamiyama, T. Kajiwara, T. Konno, T. Ito, *Inorg. Chem.* **2006**, *45*, 6460–6466.

[16] a) M. Friedrich, J. C. Gálvez-Ruiz, T. M. Klapötke, P. Mayer, B. Weber, J. J. Weigand, *Inorg. Chem.* **2005**, *44*, 8044–8052; b) E.-Q. Gao, N. Liu, A.-L. Cheng, S. Gao, *Chem. Commun.* **2007**, 2470–2472; c) L.-L. Zheng, H.-X. Li, J.-D. Leng, J. Wang, M.-L. Tong, *Eur. J. Inorg. Chem.* **2008**, 213–217.

[17] J.-P. Zhang, Y.-Y. Lin, X.-C. Huang, X.-M. Chen, *J. Am. Chem. Soc.* **2005**, *127*, 5495–5505.

[18] a) G. Rembarz, E. Fischer, K.-C. Röber, R. Ohff, H. Crahmer, *J. Prakt. Chem.* **1969**, *311*, 889–891; b) G. Götz, H. U. Kibbel, *Z. Chem.* **1975**, *15*, 278–280; c) M. Hvastijová, J. Kohout, H. Köhler, G. Ondrejovič, *Z. Anorg. Allg. Chem.* **1988**, *566*, 111–120; d) M. Hvastijová, J. Kohout, J. Klimčíková, H. Köhler, *J. Coord. Chem.* **1987**, *15*, 409–412; e) J. Mroziński, J. Kohout, M. Hvastijová, H. Köhler, *Transition Met. Chem.* **1986**, *11*, 481–484.

[19] V. Chandrasekhar, R. Azhakar, V. Krishnan, A. Athimoolam, B. M. Pandian, *J. Am. Chem. Soc.* **2006**, *128*, 6802–6803.

[20] G. R. Desiraju, T. Steiner, *The Weak Hydrogen Bond in Structural Chemistry and Biology*, Oxford University Press, Oxford, **1999**.

[21] J. Tercero, C. Diaz, J. Ribas, J. Mahía, M. A. Maestro, *Inorg. Chem.* **2002**, *41*, 5373–5381.

[22] T. Kajiwara, A. Kamiyama, T. Ito, *Chem. Commun.* **2002**, 1256–1257.

[23] *MAGMUN4.1* is freely available through http://www.ucs.mun.ca/~lthomp/magmun.html. The program may be used for scientific purposes only. Reference to it should be quoted appropriately.

[24] L. Zherlitsyna, N. Auner, M. Bolte, Y. Pozdniakova, O. Shchegolikhina, K. Lyssenko, V. Pashchenko, B. Wolf, M. Lang, F. Schütz, M. Kollar, F. Sauli, P. Kopietz, *Eur. J. Inorg. Chem.* **2007**, 4827–4838.

[25] M. F. Iskander, T. E. Khalil, W. Haase, R. Werner, I. Svoboda, H. Fuess, *Polyhedron* **2001**, *20*, 2787–2798.

[26] H. Matsushima, H. Hamada, K. Watanabe, M. Koikawa, T. Tokii, *J. Chem. Soc., Dalton Trans.* **1999**, 971–977; E. Spodine, A. M. Atria, J. Valenzuela, J. Jalocha, J. Manzur, A. M. García, M. T. Garland, O. Peña, J.-Y. Saillard, *J. Chem. Soc., Dalton Trans.* **1999**, 3029–3034.

[27] G. M. Sheldrick, *Program for Empirical Absorption Correction of Area Detector Data*, University of Göttingen, Germany, **1996**.

[28] G. M. Sheldrick, *SHELXTL*, Version 6.10, Bruker Analytical X-ray Systems, Madison, WI, USA, **2001**.

Received: May 16, 2008

Published Online: September 2, 2008